

# Crystal, Superfluid, Supersolid and Hetero-Structure in System of Two-Component Boson with Strong On-Site Repulsions in a Cubic Optical Lattice

Ikuro Ichinose, Takumi Ishima, Naohiro Kobayashi, and Yoshihito Kuno

*Department of Applied Physics, Nagoya Institute of Technology, Nagoya, 466-8555, Japan*

In the present paper, we study finite-temperature phase structure of two-component hard-core bosons in a cubic optical lattice. The system that we study in the present paper is an effective model for the Bose-Hubbard model with strong on-site repulsions and is called bosonic t-J model. This model is a bosonic counterpart of the t-J model for the strongly-correlated electron systems like the high-temperature superconducting materials. We study the model by means of path-integral methods and Monte-Carlo simulations. We found that this system has a very rich phase structure including checkerboard-type “insulating” state, superfluid, phase-separated state, inhomogeneous cloudlet state, etc. We are also interested in the possible supersolid phase with both the checkerboard order and superfluidity and found that additional nearest-neighbor inter-species attractive force induces the supersolid state. In the supersolid state, paired superfluid appears in addition to the superfluid of single atom. This result gives important insight into mechanism of the high-temperature superconductivity of the cuprate.

## I. INTRODUCTION

In the last decade, system of ultra-cold atoms has been one of the most actively studied area in atomic and condensed matter physics. Its various physical properties have been investigated quite intensively by both experimental and theoretical methods[1]. As dimensionality and interactions between particles are highly controllable and also there are no effects of impurities and defects, cold atomic system in an optical lattice is regarded as a “final simulator” for quantum many-body systems and it sometimes elevates a purely academic theoretical model to a realistic one.

It is also expected that obtained knowledge of cold atomic systems gives useful insights into physical properties of strongly-correlated many-body systems. In the present paper, we shall investigate a system of two-component bosons with strong repulsions. We shall first introduce a bosonic t-J model, which is an effective model of the Bose-Hubbard model[2] with strong on-site repulsive interactions between atoms[3]. The original t-J model of fermions is a canonical model for the high-temperature ( $T$ ) superconducting (SC) materials. The fermionic t-J model has been studied quite intensively since the discovery of the high- $T_c$  SC, but precise knowledge of its phase structure etc is still lacking partially because of difficulty of numerical study of the fermionic system. We expect that study on more tractable bosonic counterpart of the t-J model is useful to understand the strongly-correlated quantum systems including high- $T_c$  materials. This is one of our motivation to study the bosonic t-J model.

Another motivation of the present study is to see if some exotic state like the supersolid (SS), which was theoretically predicted in single-component boson systems, exists in the multi-component system. In 2004, it was reported that the SS of  $^4\text{He}$ , i.e., solid with superfluidity (SF), was observed by experiment[4]. Soon after this report, possibility of SS in cold atom systems was theoretically studied. Study of the hard-core bosons on a square lattice concluded that the realization of the SS was difficult in that system unless a long-range interaction exists[5]. On the other hand for the hard-core bosons on a triangular lattice, parameter region for possible SS state has been clarified[6]. In the SS of single-component boson, a density wave and SF coexist. In the present paper, we shall study the possibility of SS in the two-component hard-core boson systems. It should be remarked that the SS state *with paired superfluid and checkerboard order* in the bosonic system corresponds to the coexisting phase of the antiferromagnetism (AF) and SC in the electron system. Recently this AF and SC coexisting phase was really observed for highly homogeneous samples of high- $T_c$  materials[7]. Then it is quite interesting to see how the SS emerges in the present system.

This paper is organized as follows. In Sec.II, we shall briefly give the derivation of the t-J model from the Bose-Hubbard model.  $CP^1$  operators are introduced to express faithfully the hard-core nature of two-component bosons. The hard-core bosonic t-J model is studied by the mean-field theory. Obtained phase structure at the total filling factor less than unity is shown. In particular, the phase diagram contains the parameter region corresponding to the SS. In Sec.III, we study the system by means of Monte-Carlo (MC) simulations. The system in grand-canonical ensemble is studied rather in detail. At vanishing hopping of bosons, the system reduces to a spin model. This system has three phases at finite  $T$ , i.e., antiferromagnetic (AF), ferromagnetic (FM) and paramagnetic (PM) phases in terminology of spin model. Then we turn on the hopping amplitude to investigate how the SF state appears. All the above three phases result in the SF phase as the hopping amplitude is increased. We are particularly interested in phase transition from the checkerboard insulating phase (AF phase) to SF. It is verified that the phase transition is of first order with a large hysteresis loop. This result indicates that a coexisting phase of the AF solid and the SF may appear. We show that a phase separated (PS) state of the above two phases really exists at certain parameters. We investigated whether the Josephson-like tunneling of SF through AF solid takes place.

In Sec.IV, we study the system in canonical ensemble with fixed total particle number. Starting from the AF solid, we increase the hopping amplitude and study how phase of the system evolves. We found that the system behaves rather differently depending on the density of atoms. At low-density region, there exists a single second-order phase transition from the AF to SF. On the other hand for high-density region, we found another phase besides those observed in grand-canonical ensemble. This new phase is composed of SF cloudlets (finite magnitude of droplets) in the AF solid background and vice versa. The system evolves as AF crystal  $\rightarrow$  cloudlet state  $\rightarrow$  PS state  $\rightarrow$  cloudlet  $\rightarrow$  SF. Physical properties of each state are investigated by calculating correlation functions and snapshots. In Sec.V, we study effects of nearest-neighbor (NN) interaction between atoms. In particular we are interested in relation between a paired SF (PSF) [8] and AF order. In the absence of the NN interspecies attractive force, the PSF does not appear and the SF of one-body atom has no AF long-range order. However we found that by adding the NN interactions, the state with both the PSF and AF order emerges. Section VI is devoted for conclusion.

## II. MODEL HAMILTONIAN AND SLAVE-PARTICLE REPRESENTATION

As explained in the introduction, we shall study the t-J model of hard-core bosons in the cubic lattice at finite temperature[9, 10]. Hamiltonian of the t-J model is derived from the Bose-Hubbard model whose Hamiltonian is given as,

$$\begin{aligned}
 H_{\text{Hub}} = & - \sum_{r,i=1}^3 t_a (a_{r+i}^\dagger a_i + \text{h.c.}) - \sum_{r,i=1}^3 t_b (b_{r+\mu}^\dagger b_r + \text{h.c.}) + U \sum_r (n_{ar} - \frac{1}{2})(n_{br} - \frac{1}{2}) \\
 & + \frac{1}{2} \sum_{r,\alpha=a,b} V_\alpha n_{\alpha r} (n_{\alpha r} - 1) - \sum_{r,\alpha=a,b} \mu_{c\alpha} n_{\alpha r},
 \end{aligned} \tag{2.1}$$

where  $r$  denotes site of the cubic lattice,  $i(= 1, 2, 3)$  is the unit vector in the  $i$ -th direction (it also sometimes denotes the direction index), and  $a_r$  and  $b_r$  are boson annihilation operators.  $n_\alpha$  is the number operator of the boson  $\alpha$ , and therefore  $U$  and  $V_\alpha$  are inter-species and intra-species interactions, respectively. In the present paper, we shall consider the case  $t_a, t_b \ll U, V_a, V_b$ , and *the total filling factor of bosons at each site less than unity*. Furthermore we set  $t_a = t_b = t$  and  $V_a = V_b$  and also the chemical potential  $\mu_{ca} = \mu_{cb}$ . Recently studied  $^{85}\text{Rb}$ - $^{87}\text{Rb}$  atomic system is a typical

example corresponding to the present model[11]. More general cases like  $t_a \neq t_b$  will be studied in a future publication.

Effective Hamiltonian in the large on-site repulsion limit, which is called bosonic t-J model, can be obtained by the standard methods of expansion in powers of  $t/U$  and  $t/V$ ,

$$H_{tJ} = - \sum_{r,i=1}^3 t(a_{r+i}^\dagger a_r + b_{r+i}^\dagger b_r + \text{h.c.}) + J_z \sum_{r,i} S_{r+i}^z S_r^z - J_\perp \sum_{r,i} (S_{r+i}^x S_r^x + S_{r+i}^y S_r^y) - \mu_c \sum_r (1 - n_{ar} - n_{br}), \quad (2.2)$$

where pseudo-spin operator  $\vec{S}_r = \frac{1}{2} B_r^\dagger \vec{\sigma} B_r$  with  $B_r = (a_r, b_r)^t$ ,  $\vec{\sigma}$  is the Pauli spin matrices, and up to the second order of the expansion

$$J_z = \frac{4t^2}{U} - \frac{4t^2}{V}, \quad J_\perp = \frac{2t^2}{U}. \quad (2.3)$$

$\mu_c$  in Eq.(2.2) is the chemical potential of hole. In the following discussion, we shall treat  $t$ ,  $J_z$  and  $J_\perp$  as free parameters. After obtaining the critical couplings etc, we shall return to the expression (2.3) and discuss the relation to the Hubbard model. In the system  $H_{tJ}$  in Eq.(2.2), the physical state at each site  $r$  is expanded by three orthogonal basis state vectors  $\{|0\rangle, |a\rangle = a_r^\dagger|0\rangle, |b\rangle = b_r^\dagger|0\rangle\}$ , where  $|0\rangle$  is the empty state of the bosons, as multiply-occupied states have large energy because of  $U$  and  $V$ .

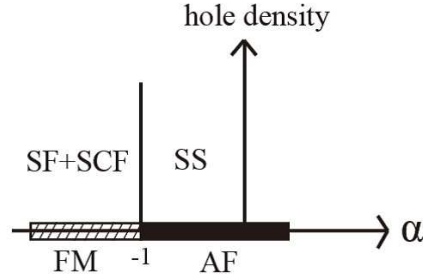


FIG. 1: Phase structure of model in  $\alpha$ -hole density plane obtained by MFT, where  $\alpha = -J_\perp/J_z$ . SCF stands for supercounter flow and SS for supersolid.

Before going into detailed numerical study on the system, it is useful to investigate the groundstate properties of the model by the mean-field theory (MFT). We use a variational wave function of bosons that has a site-factorized form,

$$|\Psi\rangle = \prod_r \left[ \sin \frac{\theta_r}{2} \left( \sin \frac{\chi_r}{2} a_r^\dagger + \cos \frac{\chi_r}{2} b_r^\dagger \right) + \cos \frac{\theta_r}{2} \right] |0\rangle. \quad (2.4)$$

It is straightforward to calculate the expectation value of the Hamiltonian  $H_{tJ}$  (2.2) in the state  $|\Psi\rangle$ . From  $E_{tJ} = \langle H_{tJ} \rangle$ , we can obtain a phase diagram of the bosonic t-J model at vanishing temperature ( $T$ ). Details have been already published in the previous paper[3], and therefore here we only show the phase diagram in Fig.1. At the total filling factor unity, the system  $H_{tJ}$  reduces to the spin model, the anisotropic Heisenberg model. We introduce parameter  $\alpha = -J_\perp/J_z$  for the anisotropy. At  $\alpha = -1$ , phase transition takes place, and for  $\alpha > -1$  antiferromagnetic (AF) phase appears whereas for  $\alpha < -1$  ferromagnetic (FM) phase is realized. For the original atomic model,

AF phase corresponds to the state with the checkerboard symmetry of  $a$  and  $b$  atoms. On the other hand, the FM long-range order (LRO) means nonvanishing condensation  $\langle a_r^\dagger b_r \rangle \neq 0$ , and sometimes it is called supercounter flow (SCF) in the original atomic system. As holes are doped, SF state with single-atom condensation  $\langle a_r \rangle = \langle b_r \rangle \neq 0$  takes place. In particular, the state with AF+SF is called supersolid (SS) as it has not only the checkerboard symmetry but also off-diagonal LRO of SF.

For numerical calculation, it is necessary to express the constrained Hilbert space faithfully. To this end, we introduce the following slave-particle representation as in the previous paper[3],

$$a_r = \phi_r^\dagger c_{r1}, \quad b_r = \phi_r^\dagger c_{r2}, \quad (2.5)$$

$$\left( \phi_r^\dagger \phi_r + c_{r1}^\dagger c_{r1} + c_{r2}^\dagger c_{r2} - 1 \right) |\text{phys}\rangle = 0, \quad (2.6)$$

where  $\phi_r$  is a hard-core boson and  $c_{r\ell=1,2}$  is an ordinary boson. Equation (2.6) is the local constraint on the physical state. From Eq.(2.5), the hard-core boson  $\phi_r$  creates the empty state of the original bosons  $a_r$  and  $b_r$ , whereas  $c_{r1}$  ( $c_{r2}$ ) creates the state of  $a_r^\dagger|0\rangle$  ( $b_r^\dagger|0\rangle$ ), i.e.,

$$|0\rangle \leftrightarrow \phi_r^\dagger |\Omega\rangle, \quad a_r^\dagger |0\rangle \leftrightarrow c_{r1}^\dagger |\Omega\rangle, \quad b_r^\dagger |0\rangle \leftrightarrow c_{r2}^\dagger |\Omega\rangle, \quad (2.7)$$

where  $|\Omega\rangle$  is the empty state of the slave particles.

In order to express the local constraint (2.6) in more convenient way, we introduce a  $\text{CP}^1$  boson (the Schwinger boson)  $z_{r\ell}$ ,

$$c_{r\ell} = (1 - \phi_r^\dagger \phi_r) z_{r\ell}, \quad (\ell = 1, 2) \\ \left( \sum_{\ell=1,2} z_{r\ell}^\dagger z_{r\ell} - 1 \right) |\text{phys}\rangle_z = 0. \quad (2.8)$$

It is easily verified that Eq.(2.6) is satisfied by Eq.(2.8). The hard-core boson  $\phi_r$  itself can be expressed in terms of another  $\text{CP}^1$  boson  $w_{r\ell}$  as follows,

$$\phi_r = w_{r2}^\dagger w_{r1}, \quad \left( \sum_{\ell=1,2} w_{r\ell}^\dagger w_{r\ell} - 1 \right) |\text{phys}\rangle_w = 0. \quad (2.9)$$

It is easily verified  $[\phi_r, \phi_r^\dagger]_+ = 1$ , and operators  $\phi_r^\dagger$ ,  $\phi_{p \neq r}$  etc commute with each other. From Eq.(2.9), it is obvious that  $|0\rangle_\phi = w_{r2}^\dagger |0\rangle_w$  and  $\phi_r^\dagger |0\rangle_\phi = w_{r1}^\dagger |0\rangle_w$ . The effective Hamiltonian  $H_{\text{tJ}}$  can be easily expressed in terms of the  $\text{CP}^1$  bosons  $z_{r\ell}$  and  $w_{r\ell}$ .

### III. SYSTEM IN GRAND-CANONICAL ENSEMBLE: MONTE-CARLO SIMULATIONS

In this section, we show the results of study on the system in the grand-canonical ensemble(GCE). In the cold atom system in an optical lattice, the system in the GCE corresponds to the case of nearly flat confining potential. See Fig.2. Generally speaking, around a first-order phase transition point at which particle density changes drastically, very subtle adjustment of the chemical potential is required to obtain a desired particle density. Study of the system in the canonical ensemble (CE) with fixed particle density is complementary and helpful for investigation of first-order phase transition. In the present paper, the study of the system in the CE will be reported in the following section.

Partition function of the system in the GCE at temperature  $T$ ,  $Z_{\text{GCE}}$ , is given by the path-integral methods as follows[3],

$$Z_{\text{GCE}} = \int [D\bar{w} Dw D\bar{z} Dz] e^{-\beta H_{\text{tJ}}(\bar{w}, w, \bar{z}, z)}, \quad (3.1)$$



FIG. 2: Physical picture of GCE, in which density of atoms is controlled by chemical potential.

where  $\beta = 1/(k_B T)$  and the Hamiltonian  $H_{tJ}(\bar{w}, w, \bar{z}, z)$  is obtained from  $H_{tJ}$  in Eq.(2.2) by substituting the  $CP^1$  variables  $z_r$  and  $w_r$  for the  $CP^1$  operators. We have numerically studied the system (3.1) and obtained phase diagram etc for various values of the chemical potential  $\mu_c$ . In order to identify a phase boundary, we measured the “internal energy”  $E$  and the specific heat  $C$ , which are defined as

$$E = \frac{1}{L^3} \langle \beta H_{tJ}(\mu_c = 0) \rangle, \quad C = \frac{1}{L^3} \langle (\beta H_{tJ}(\mu_c = 0) - E)^2 \rangle, \quad (3.2)$$

where  $L$  is the linear system size. We impose the periodic boundary condition for practical calculation. We often use the following *dimensionless parameters* for describing phase diagram etc,

$$c_1 = \beta J_z, \quad c_3 = \beta t, \quad \alpha = -J_\perp/J_z. \quad (3.3)$$

#### A. Phase diagram

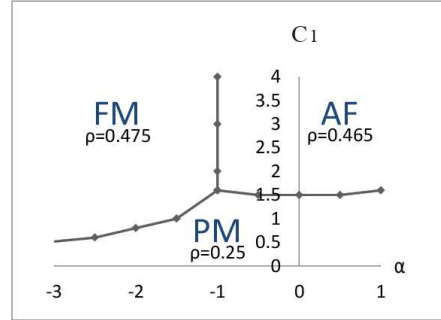


FIG. 3: Phase structure of model for  $t = \mu_c = 0$  in  $\alpha - c_1$  plane, where  $\alpha = -J_\perp/J_z$  and  $c_1 = \beta J_z$ . There are three phases, PM, AF and FM phases. Physical meaning of each phase is explained in the text. Typical value of particle density  $\rho = \langle a_r^\dagger a_r \rangle = \langle b_r^\dagger b_r \rangle$  in each phase is also shown.

We first consider the case of  $t = 0$ , i.e., the system without particle hopping. In Fig.3, we show the obtained phase diagram in the  $\alpha - c_1$  plane for  $\mu_c = 0$  and  $c_1 > 0$ . Details of the calculation have been already reported in the previous paper[3]. Similar phase diagrams are obtained for other values of  $\mu_c$ . There are three phases, paramagnetic (PM),  $z$ -component-AF and  $xy$ -component-FM phases. At high- $T$ , the system is in the PM phase without any long-range order, as it is expected. As  $T$  is lowered, phase transition to the AF or FM phase takes place. The AF state corresponds to the checkerboard state and the FM state to the state with the SCF  $\langle a_r^\dagger b_r \rangle \neq 0$ , as we explained previously. These phase transitions are of second order. In the low- $T$  region, there exists a line of the phase boundary between the AF and FM phases at  $\alpha = -1$  as predicted by the MFT. On the line  $\alpha = -1$ , the pseudo-spin symmetry is enhanced to  $SU(2)$  as the inter-species and intra-species interactions between atoms are the same, otherwise the symmetry is  $U(1) \times Z_2$ , i.e., global rotation of  $(S_r^x, S_r^y)$  and reflection  $S_r^z \rightarrow -S_r^z$ . The enhancement of the symmetry is seen by the redefinition

of operators as  $a_r \rightarrow -a_r$  for  $r \in \text{odd site}$ . By this redefinition,  $(S_r^x, S_r^y) \rightarrow -(S_r^x, S_r^y)$  for  $r \in \text{odd site}$ , and then  $J_\perp \rightarrow -J_\perp$ . For ferroelectric materials, similar transition line to the present  $\alpha = -1$  one is called a morphotropic phase boundary and plays a very important role[12].

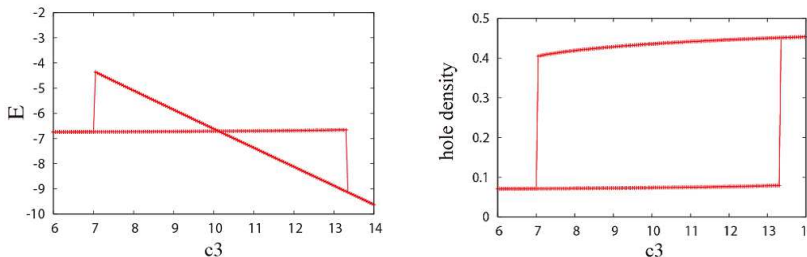


FIG. 4: Internal energy and hole density as a function of  $c_3 = \beta t$  for  $c_1 = 3.0$  and  $\alpha = -0.5$ . Phase transition from AF state to SF is of first order.

Let us turn on the hopping amplitude  $t$ . We choose typical three points in the  $\alpha$ - $c_1$  plane for each of the three phases existing at  $t = 0$ , and investigated how the phases change as the value of  $c_3 = \beta t$  is increased. We have found that all of the three phases make phase transition to the SF phase. In Fig.4, we show  $E$  and hole density for the phase transition from the AF phase to SF. These results were obtained by the MC simulations of local-update Metropolis algorithm. More elaborate update methods slightly decreases the region of the hysteresis loop[3]. Anyway from the above calculations, it is obvious that the phase transition is of first order. To verify the finite superfluidity, we calculated the boson correlation function  $\langle B_0^\dagger \cdot B_r \rangle$ , and found it has a nonvanishing correlation as  $r \rightarrow \text{large}$  after the phase transition. We also have measured the spin correlation function and found that SF phase has a FM spin correlation. Physical meaning of the appearance of the FM correlation has been explained in the previous paper[3](see also discussion in Sec.IV). Emergence of the first-order phase transition stems from the fact that both of the phases separated by the phase transition have the LRO's, i.e., the AF and SF+FM orders, respectively.

Existence of the first-order phase transition gives an interesting possibility of various (metastable) phases in the parameter region of hysteresis loop, e.g., (i) phase separation (PS) of AF state and SF, (ii) supersolid with coexistence of the global AF order and SF, (iii) immiscible state of the AF and SF cloudlets without any genuine LRO. We have studied the above problem in both the GCE and the canonical ensembles. In the GCE of a constant chemical potential, in which the average number density is *not* conserved as the parameters vary, we have found that in most of the parameter region only one of the AF solid or SF is stable in the *flat potential* with  $\mu_c = \text{constant}$ , and the values of parameters  $t$  and  $\mu_c$  control which phase appears. In fact, we choose an inhomogeneous state as an initial state and update the configuration by means of the standard Metropolis algorithm. After  $10^5$  updates, the whole system tends to become either the AF state with checkerboard order or the SF with intermediate homogeneous hole density. Only at very specific value of  $c_{3c} = 9.362$ , the stable PS state of the AF and SF phases appears. This means that the genuine first-order phase transition takes place at  $c_{3c} = 9.362$ , and the system is composed of immiscible AF and SF domains at the phase transition point.

Here one should remark that the phase transition takes place at  $\beta \frac{t^2}{U}$ ,  $\beta \frac{t^2}{V} \sim O(1)$  and  $\beta t \sim O(10)$ . Then  $\frac{t}{U}$ ,  $\frac{t}{V} \sim O(\frac{1}{10})$ . This means that the phase transition observed above in the t-J model also exists in the original Hubbard model.

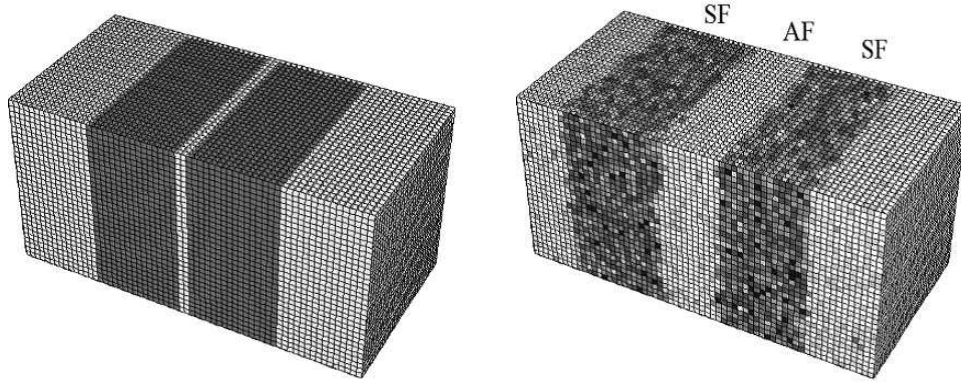


FIG. 5: Heterojunction of SF and AF state. (Left) Initial state before update. (Right) After  $8 \times 10^5$  sweeps. The central *bright* region is the AF solid state with *high particle density*, whereas the *dark* regions represent state of *high hole density*. Confining potential with  $\Lambda = 40$  and  $N_\ell = 2$ .

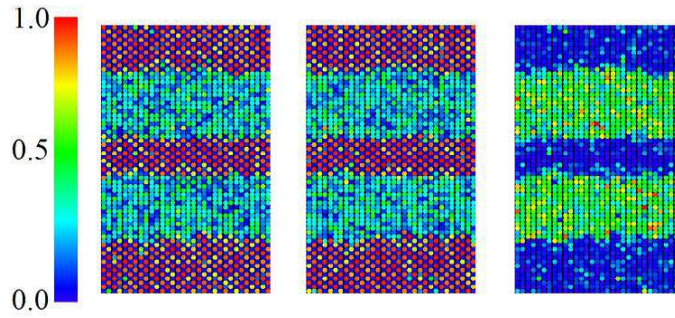


FIG. 6: Snapshots in a horizontal plane of heterojunction of SF and AF state in Fig.5. (Left) Density of *a*-atom (Center) Density of *b*-atom (Right) Density of hole. It is obvious that *a* atom and *b* atom reside on each sublattice in the AF region.

### B. Heterojunction of superfluid and AF crystal

In the previous subsection, we showed that both the AF and SF states can coexist at the first-order phase transition region. In the GCE with constant chemical potential  $\mu_c$ , either the AF or SF state is realized as a “homogeneous” state except at the genuine critical coupling  $c_{3c} = 9.362$ . However in the confinement potential of real experiments, the density of the atoms is inhomogeneous. In the central region in which the atomic density is higher, the AF state is expected to appear, whereas in the outer region the SF state with a lower atomic density is expected to appear. If the inhomogeneous PS state is realized around the first-order phase transition point, it resembles to the classical solid-fluid PS state like coexisting state of ice and water. However as the present system is a quantum system, one may expect that some interesting and characteristic phenomena of macroscopic quantum system occur in such a coexisting state. One example is a kind of the Josephson tunneling in a heterojunction of the AF “crystal” state and SF. In the present case, the both AF state and SF are made of *a* and *b* atoms. Therefore, to study physical properties of heterojunction of these states is very interesting.

In this section, we study the above problem by means of MC simulations. To specify spatial direction of the AF layer, we introduce a certain inhomogeneity in terms of the chemical potential  $\mu_c$ . In the practical calculation, we make an AF layer parallel to the *y-z* plane at  $x \sim 0$  by adjusting chemical potential as  $\mu_c = \Lambda(>0)$  for  $x = 0, \pm 1, \dots, \pm N_l$ , and otherwise zero. As expected, a stable AF layer is generated after the MC local update of the system. We show some example in Figs.5



and 6. Please notice that we employ the periodic BC.

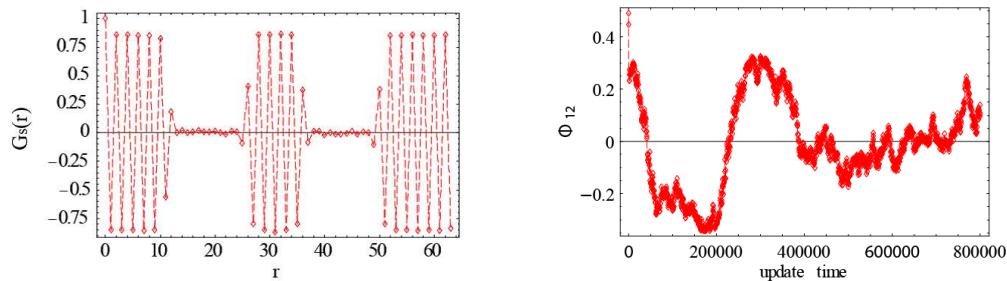


FIG. 7: Physical properties of heterojunction of SF and AF state. (Left) Spin correlation  $G_S^{\perp}(r)$ . There exists no spin correlations in SF region. (Right) Phase difference  $\Phi_{12}$  of Bose condensates in two SF regions as a function of update. It fluctuates strongly.

We first show the spin correlation function

$$G_S^{\perp}(r) = \langle \vec{S}_{r_0} \cdot \vec{S}_{r_0+r} \rangle, \quad (3.4)$$

where the site  $r_0$  is located in one of the AF layers and  $r$  is a lattice vector perpendicular to the AF and SF layers. It is obvious that there exist no pseudo-spin correlations in the SF regions, whereas in the AF regions the checkerboard configurations of  $a$  and  $b$  atoms are realized.

In this PS state, it is interesting to investigate if the tunneling of SF current takes place through the AF layer. To study this problem, we measured the correlation function of the bosons through the intermediate AF layer. If there exists a finite correlation between SF states separated by the AF layer, “Josephson tunneling” occurs as in the SC-insulator heterojunction. In Fig.7, we show the result of the atomic SF correlation  $\Phi_{12}$  that is defined as

$$\Phi_{12} = \text{Im} \left[ \log \left( \langle B_{r_1}^{\dagger} \cdot B_{r_2} \rangle \right) \right], \quad (3.5)$$

where  $r_1$  ( $r_2$ ) is located inside of the left (right) SF layer in Fig.5. It is obvious that correlation of two SF states fluctuates randomly in the MC update. We examined some other cases and obtained similar results. This result is unexpected because both the AF state and SF are made of  $a$  and  $b$  atoms and then it is expected that atoms move almost freely through the interface. In order words, there exists a sharp boundary between the two states and the “classical state”, i.e., the AF crystal, and the quantum state, i.e., SF, have very different properties.

#### IV. PHASE SEPARATION AND INHOMOGENEOUS STATES IN CANONICAL ENSEMBLE: MONTE-CARLO SIMULATIONS

In the previous section, we studied the system in the GCE with fixed chemical potential. In particular we are interested in the AF phase and SF that are separated by the first-order phase transition. In the GCE, in most of the parameter region it is observed that only homogeneous AF state or SF state is stable. However in the previous studies on some related systems like hard-core bosons on a triangular lattice, the PS state is observed in the CE even if it is not found in the GEC[6]. This result stems from the fact that the CE corresponds to the physical situation of fixed averaged particle density and therefore atoms are assumed to be confined in a certain flat region with a sharp boundary like a box, see Fig.8. Then it is interesting to study the present system in the CE and see if a SS state or some related state exists in some parameter region.



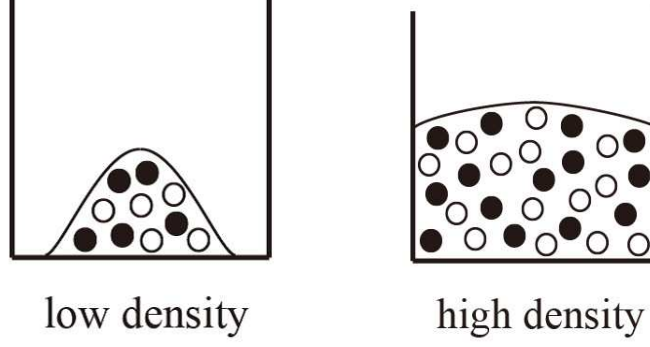


FIG. 8: Physical picture of CE, in which density of atoms is fixed.

### A. Low-density region

By the practical calculation, we found that the system's physical behaviors, including phase structure itself, changes as the average particle density varies. In this subsection, we study the system with average atomic density  $\rho_a = \rho_b = 15\%$  and the system size  $L = 24$ . This case corresponds to the low-density region. For small hopping amplitude  $t$  and  $\alpha > -1$ , it is expected that the system at low  $T$  tends to separate into the AF solid and “empty” region, as the Boltzmann factor dominates the entropy factor at low  $T$ . As the hopping amplitude  $t$  is increased, a phase transition to the SF is expected to occur as observed by the simulations in the GCE in the previous section. This expectation has been confirmed by the MC simulations.

We first consider the case  $c_1 = 5$  and  $\alpha = -0.5$ , relatively large value of  $J_z$ . For small hopping amplitude  $t$ , the system exists in the AF phase. As  $t$  is increased, a phase transition takes place at  $c_3 \simeq 6.0$ . See Fig.9, in which internal energy and specific heat of each term in  $H_{tJ}$  in (2.2) are shown. It is useful to see snapshot of the system before and after the phase transition. See Fig.10. It is obvious that holes (i.e., atoms) are localized and make some domain at  $c_3 = 0$ , whereas particles are homogeneously distributed for  $c_3 = 8$ .

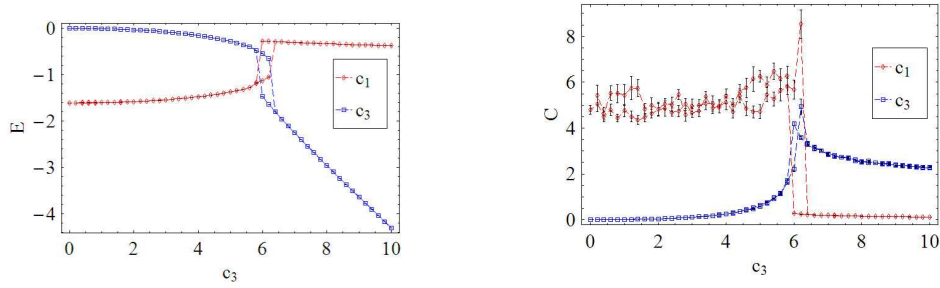


FIG. 9: Internal energy and specific heat of  $c_1$  and  $c_3$  terms as a function of  $c_3$  for system with  $\rho_a = \rho_b = 15\%$  in CE. Results show existence of first-order phase transition at  $c_3 \simeq 6.0$ .

To verify that the observed phase transition is a transition from the AF crystal to SF, we calculated the correlation function of the boson operator  $B_r = (a_r, b_r)^t$ ,

$$G_{\text{SF}}(r) = \frac{1}{L^3} \sum_{r_0} \langle B_{r_0}^\dagger \cdot B_{r_0+r} \rangle. \quad (4.1)$$

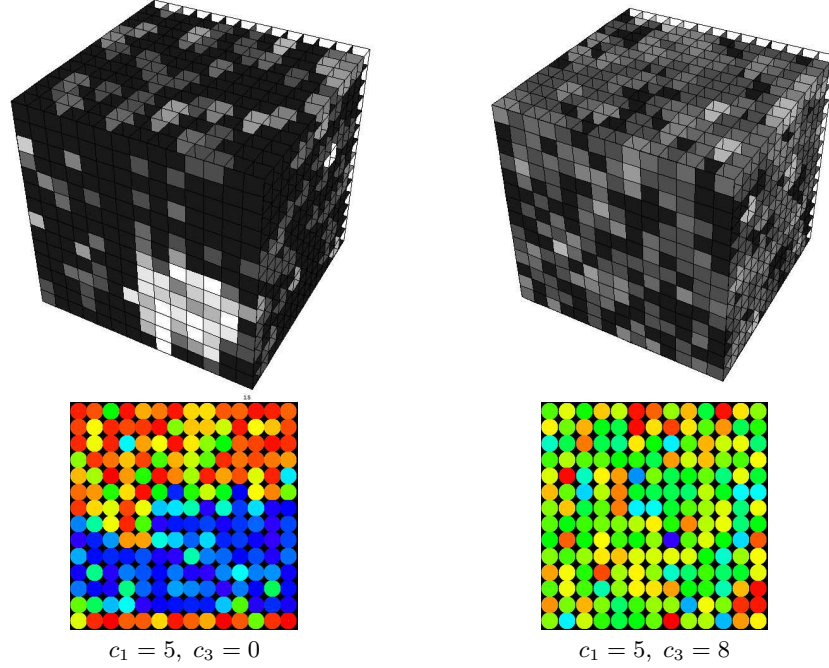


FIG. 10: Snapshot of density of holes in the system with  $\rho_a = \rho_b = 15\%$  before ( $c_3 = 0$ ) and after ( $c_3 = 8$ ) the phase transition at  $c_3 \simeq 6.0$ .  $c_1 = 5.0$ . Bright (dark) region represents region of high (low) atomic density. In the low-hopping region, system is divided into AF and empty regions. On the other hand in the high-hopping region, homogeneous SF state is realized. The phase transition is of first order.

We also calculated the spin correlation function,

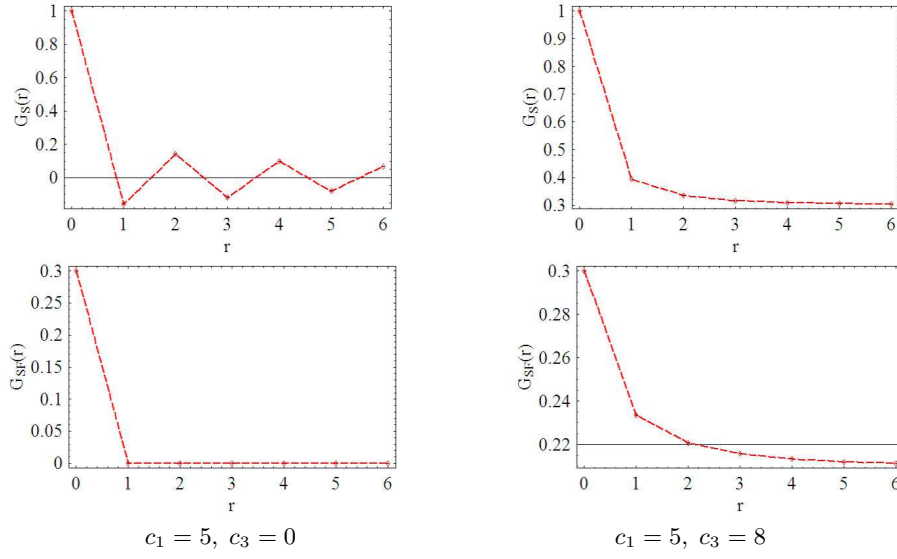
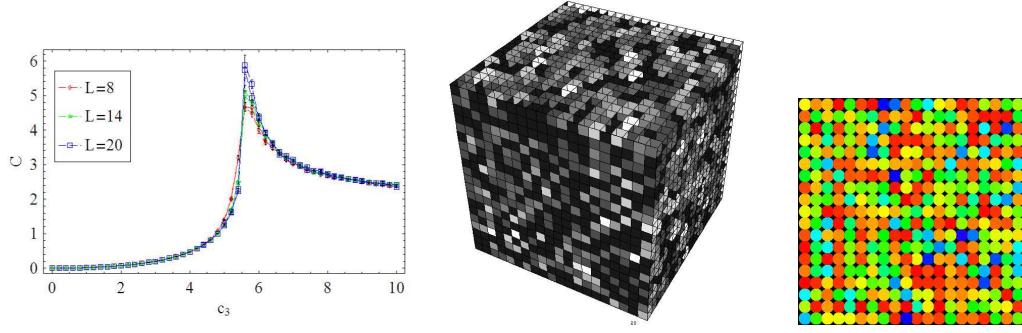
$$G_S(r) = \frac{1}{L^3} \sum_{r_0} \langle \vec{S}_{r_0} \cdot \vec{S}_{r_0+r} \rangle. \quad (4.2)$$

Results are shown in Fig.11. It is obvious that the SF phase transition at  $c_3 \simeq 6.0$  accompanies a transition from the AF to FM in the spin degrees of freedom. As explained in the previous paper[3], it should be remarked that the FM order in the SF state is a natural outcome of the two-component SF and it should not be regarded as the genuine FM order in the magnetism. In fact, the wave function of the  $a$  and  $b$ -atomic SF is well-described by the following MFT-type wave function,

$$|\text{SF}\rangle = \prod_r \left[ \sin \frac{\theta}{2} \left( \frac{1}{\sqrt{2}} a_r^\dagger + \frac{1}{\sqrt{2}} e^{i\phi} b_r^\dagger \right) + \cos \frac{\theta}{2} \right] |0\rangle, \quad (4.3)$$

where we have assumed the translational symmetry and recovered the relative phase between  $a$  and  $b$  SF condensates,  $e^{i\phi}$ , which was ignored in Eq.(2.4). By using Eq.(4.3), it is straightforward to calculate expectation value of the pseudo-spin operator  $\vec{S}_r$  to find that the state  $|\text{SF}\rangle$  exhibits the FM order.

We also studied the low-density case with  $c_1 = 3$  and  $\alpha = -0.5$ , relatively small value of  $J_z$ . Calculation of the specific heat  $C$  is shown in Fig.12.  $C$  has a system-size dependence, which indicates that the phase transition at  $c_3 \simeq 5.5$  is of second order. We also show snapshots of hole density for  $c_3 = 0$ . Compared with the case of  $c_1 = 5$ , atoms are distributed rather homogeneously. We verified that spin correlation function  $G_S(r)$  in that region has no LRO. This is the reason why the phase transition turns to second order. The result suggests existence of the tricritical point at which the phase transition changes from second to first one as  $c_1$  is increased.

FIG. 11: Correlation functions  $G_{\text{SF}}(r)$  and  $G_{\text{S}}(r)$ .FIG. 12: Specific heat  $C$  for  $\rho_a = \rho_b = 15\%$  with  $c_1 = 3$  as a function of  $c_3$ . There exists a second-order phase transition at  $c_3 \simeq 5.5$ . We also show snapshots for  $c_3 = 0$ . Compared with the case of  $c_1 = 5$ , system in the low-hopping region is rather homogeneous.

### B. High-density region

In this subsection, we study the system with average atomic density  $\rho_a = \rho_b = 38\%$  with  $c_1 = 3$  and the system size  $L = 24$ . This case is close to that observed by the GCE in the previous section and corresponds to the high-density region, see Fig.8. Numerical study of the internal energy  $E$  and the specific heat  $C$  indicates the existence of (at least) three phase transitions as shown in Fig.13. All of them are of first order as the density of state  $N(E)$  has a double-peak shape as shown in Fig.14, where  $N(E)$  is defined as

$$\begin{aligned} Z_{\text{CE}} &= \int_{\text{CE}} [D\bar{w}DwD\bar{z}Dz] e^{-\beta H_{\text{tJ}}(\bar{w}, w, \bar{z}, z)}, \\ &= \int dE e^{-\beta E} N(E). \end{aligned} \quad (4.4)$$

In Eq.(4.4),  $\int_{\text{CE}}$  denotes the integration over configurations with a fixed number of atoms (or fixed average density of atoms), and  $N(E)$  is a function of  $\beta$  and coupling constants. Furthermore from  $c_3 \simeq 13$  to  $c_3 \simeq 15$ , there is a large hysteresis loop in  $E$  indicating existence of at least one first-order

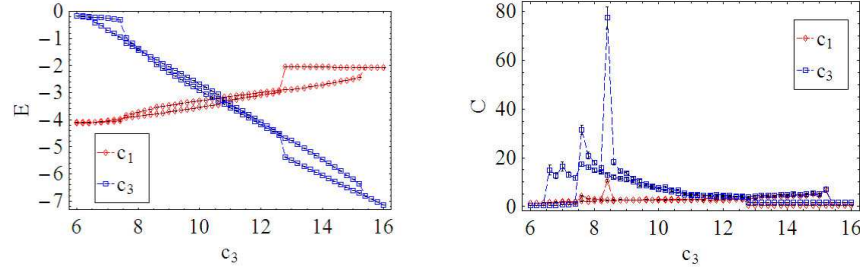


FIG. 13: Internal energy and specific heat of each term in  $H_{tJ}$  measured in CE as a function of  $c_3$ .  $\rho_a = \rho_b = 38\%$  with  $c_1 = 3$ . There are three phase transition s at  $c_3 = 7.6, 8.4$ , and  $14.5$ .  $L = 24$ .

phase transition. It is obvious that the system with high particle density has a rather complicated phase structure compared with the low-density case.

Snapshot of system at various  $c_3$  is quite useful to understand physical meaning of various phases. See Fig.15. At  $c_3$  is increased from zero, a transition from the AF checkerboard state to a new phase takes place. This new phase is inhomogeneous and composed of immiscible AF solid region and SF droplet of macroscopic magnitude (i.e., cloudlet). The appearance of this coexisting phase comes from the fact that the AF and SF states tend to have a sharp interface as we saw in the previous section. At the second phase transition, a complete PS takes place and the system is divided into the AF and SF phases. Width of each phase is determined by the atomic density  $\rho$  and the hopping amplitude  $c_3$ . As the value of  $c_3$  is increased furthermore, a transition to an inhomogeneous phase composed of immiscible SF region and AF cloudlet takes place. Finally for large  $c_3$ , the phase transition into the homogeneous SF takes place.

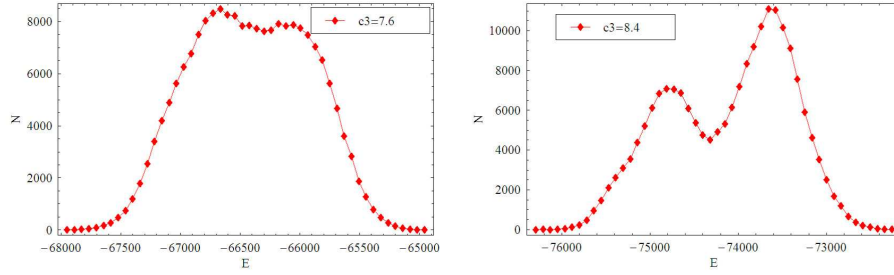


FIG. 14: Histograms of  $N(E)$ . They have double-peak shape, which indicates the first-order phase transition.

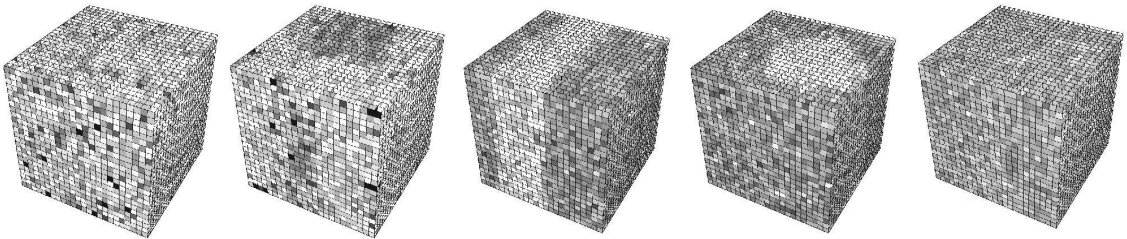


FIG. 15: Snapshot of system at various values of  $c_3$ . (From left to right)  $c_3 = 7, 8, 10.6, 12$  and  $16$ . Bright (dark) region corresponds to higher (lower) atomic density.

It is also interesting to see how the pseudo-spin correlation function behaves for various values of  $c_3$ . We show the results in Fig.16. For  $c_3 = 6$ , the system exists in the AF phase, and for  $c_3 = 16$



the system is in the SF phase and the pseudo-spin correlation has a FM order. In the intermediate regions, the pseudo-spin correlation is a superposition of the AF and FM LRO's. Similar behavior has been observed in other systems by the previous study[13]. It should be remarked that even in the SP states, the correlation functions averaged over positions and directions do not exhibit any singular behavior that indicates the existence of sharp phase boundary.

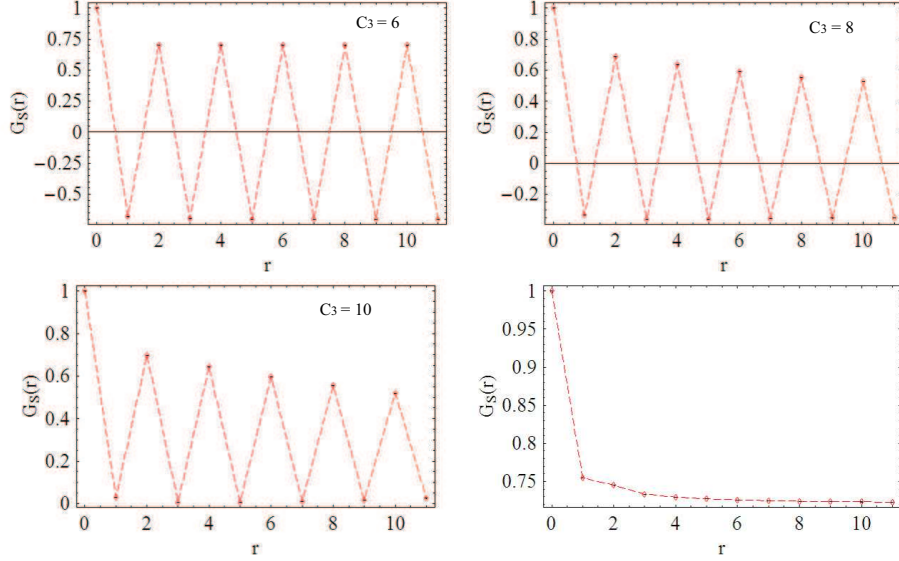


FIG. 16: Pseudo-spin correlation for  $c_3 = 6, 8, 10$  and  $16$ . In the states of mixture of AF solid and SF for  $c_3 = 6, 8, 10$ , pseudo-spin correlation is a superposition of AF and FM, whereas in the SF, LRO of FM is realized.

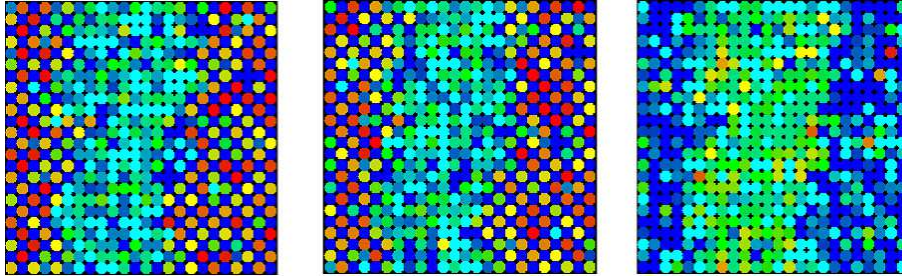


FIG. 17: Snapshots of density of  $a$ -atoms (left),  $b$ -atom (center) and holes (right) in PS state for  $c_3 = 7.6$ .

In Fig.17, we show snapshots of density of  $a$  atom,  $b$  atom and hole for  $c_3 = 7.6$ . It is clear that in the AF region, checkerboard configuration of  $a$  and  $b$  atoms is realized. On the other hand in the SF region, liquid-like distribution of holes is realized. In fact, in each snapshot, there is a small fluctuation of hole density in the SF phase, but after averaging over various snapshots (configurations), hole density has a quite homogeneous distribution.

It is interesting to see how SF is realized in each phase. In order to study it, we calculated the correlation function of atoms  $G_{SF}(r)$ . (It is obvious that  $G_a(r) = G_b(r)$  in the present case.) We show the results in Fig.18. The result shows that in the AF phase the correlation tends to vanish very rapidly (no correlation even in the NN pair), and in the SF phase it has a genuine LRO. In the PS state, the correlator seems to have a small but finite LRO, but its finiteness comes from the correlation in the SF layers. Then the above results are consistent with the observation by the GCE in the previous section, which indicates that the SF correlation terminates at AF layers.

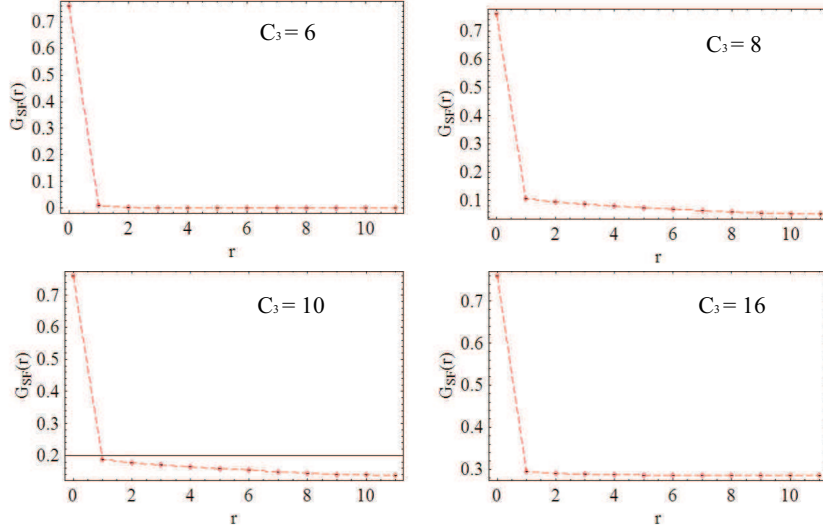


FIG. 18: Correlation functions of atoms  $G_{\text{SF}}(r)$  for  $c_3 = 6, 8, 10$  and  $16$ .

### V. EFFECTS OF NN INTERACTIONS AND PAIRED SUPERFLUID

In this section, we shall study effects of NN attractive force between  $a$  and  $b$  atoms and investigate the possibility of the PSF. This problem is closely related to the strongly-correlated electron systems and superconductivity of the cuprates. The high- $T_c$  materials are hole-doped AF magnets, and a hole pair sitting on NN sites feels attractive force due to (short-range) AF background. It is widely believed that this attractive force is an origin of the superconductivity. Then it is very interesting to study if the PSF is realized in the present system besides the single-atom SF.

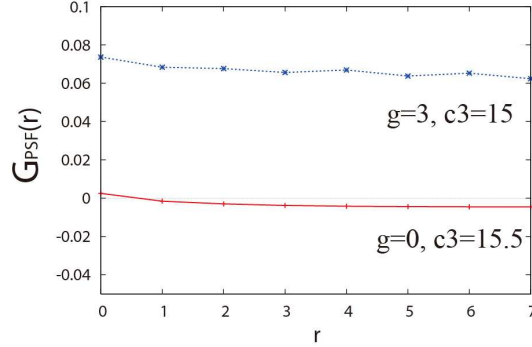


FIG. 19: Correlation function of PSF in the cases  $g = 0$  and  $g = 3$  for  $\rho_a = \rho_b = 34\%$ . Results indicate existence of small but finite LRO for  $g = 3$ , whereas no PSF for  $g = 0$ .

Existence of the PSF is examined by measuring the following correlation function,

$$G_{\text{PSF}}(r) = \frac{1}{3} \sum_i \left( \langle (a_r^\dagger b_{r+i}^\dagger)(a_0 b_i) \rangle - \langle a_r^\dagger a_0 \rangle \langle b_{r+i}^\dagger b_i \rangle \right). \quad (5.1)$$

We show the calculation of  $G_{\text{PSF}}(r)$  for  $\rho_a = \rho_b = 34\%$  in Fig.19. The result obviously indicates that there is no finite density of the PSF in the system  $H_{\text{tJ}}$ .

Then we have studied effects of interaction between a pair of atoms on NN sites by adding the following term to the Hamiltonian,

$$\beta H_{\text{NN}} = -g \sum_{r,i} \left( (a_r^\dagger a_r)(b_{r+i}^\dagger b_{r+i}) + (b_r^\dagger b_r)(a_{r+i}^\dagger a_{r+i}) \right). \quad (5.2)$$

Experimental realization of “long-range” interactions like (5.2) in cold atom system was recently discussed[14]. We have investigated the *extended t-J model*  $H_{\text{tJ}} + H_{\text{NN}}$  with fixed value of  $g$ . First for  $c_3 = 0$  and positive  $g$ , similar phase diagram to that of  $c_3 = g = 0$  in Fig.3 is obtained but the parameter region of the AF state is enlarged as a result of  $H_{\text{NN}}$ .

We are again interested in how the AF state evolves as the hopping parameter  $c_3$  is increased. As in the case of  $g = 0$  considered in the previous section, we shall study the low and high-density cases separately.

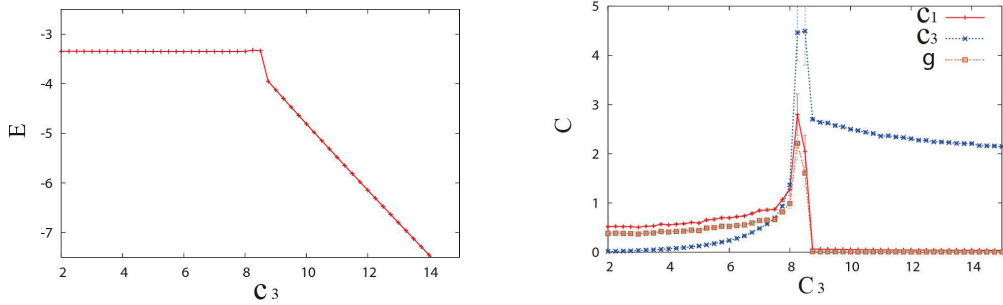


FIG. 20: System of  $\rho_a = \rho_b = 15\%$ . Internal energy  $E$  and specific heat  $C$  as a function of  $c_3$  for  $g = 3$ ,  $c_1 = 3.0$  and  $\alpha = -0.5$ . In  $C$ , “specific heat of each term” is shown.

#### A. Low-density region

In this subsection, we consider the case with  $\rho_a = \rho_b = 15\%$  and  $g = 3$ . We show  $E$  and  $C$  as a function of  $c_3$  in Fig.20. It is obvious that there exists a first-order phase transition at  $c_3 \simeq 8.5$ . For small  $c_3$ , the system is divided into empty state and AF crystal as in the case  $g = 0$ , and after the phase transition the homogeneous SF state appears. See Fig.21. In the SF phase, we calculated  $G_{\text{SF}}(r)$  and  $G_{\text{PSF}}(r)$  and we show the result in Fig.22. We also calculated  $G_{\text{S}}(r)$ . It is obvious that no PSF is generated and FM LRO for pseudo-spin correlation is formed in the SF. This means that effect of the NN attractive force is negligibly small in the low-density region.

#### B. High-density region

We studied the system with atomic density  $\rho_a = \rho_b = 34\%$  by the MC simulation in the CE. In Fig.23, we show the specific heat  $C$  as a function of  $c_3$  for  $g = 3$ . The result shows that there are three phase transitions. We have verified that all of them are second-order phase transitions. We also show the SF and the PSF correlation functions in Fig.24 (see also Fig.19). Contrary to the case  $g = 0$ , all SF correlations have finite LRO after the first phase transition at  $c_3 \simeq 10.8$ . Small but finite LRO of the PSF exists in all phases except the AF phase.

One may think that this difference in the SF behavior between in the  $g = 0$  and  $g = 3$  cases, in particular (non)existence of the PSF, is related to different behavior of pseudo-spins in the two



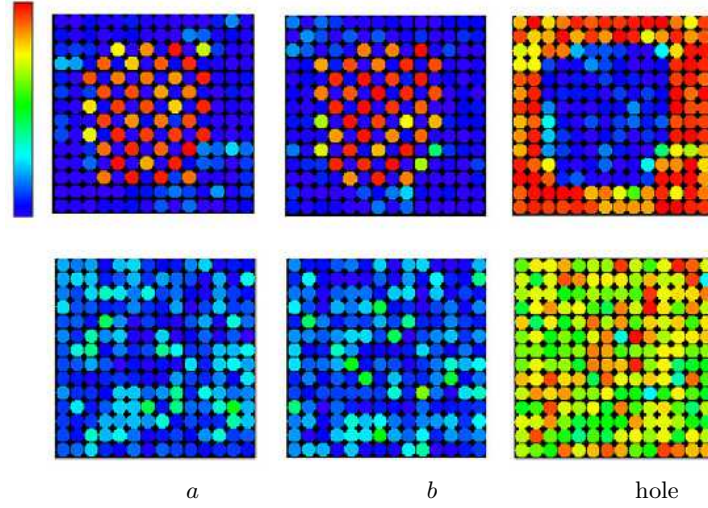


FIG. 21: Snapshots  $c_3 = 0$  (upper panels) and  $c_3 = 8$  (lower panels) in low-density region and  $g = 3$ .

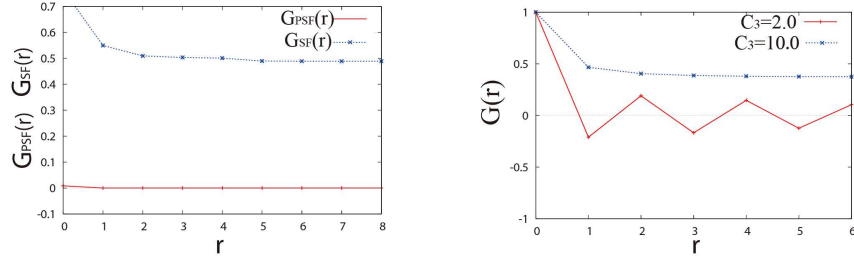


FIG. 22:  $G_{SF}(r)$  and  $G_{PSF}(r)$  (Left panel).  $G_S(r)$  (Right panel). In the SF with low-atomic density, no PSF is generated and FM RLO for pseudo-spin correlation is formed.

cases. Then we studied the pseudo-spin correlation and obtained the results shown in Fig.25, where

$$G_{xy}(r) = \frac{1}{L^3} \sum_{r_0} \sum_{i=x,y} \langle S_{r_0}^i S_{r_0+r}^i \rangle. \quad (5.3)$$

As expected, in the model  $g = 3$  there exists AF correlation in  $z$ -component, besides the FM correlation in  $xy$ -component. We also studied the snapshots of each phase, which are quite helpful for understanding properties of phases. From these results, we found that the PS takes place even in the AF state for  $c_3 < 10.8$ . However in the present case, the phase is separated into empty phase with very low particle density and the AF phase of checkerboard symmetry. The intermediate two phases, the AF solid and SF coexist but *they are immiscible*. On the other hand for  $c_3 > 14.3$ , the global domain structure disappears. It is very interesting to see if the SS state is realized due to the NN coupling  $H_{NN}$  in Eq.(5.2). Some previous study on the single-band Hubbard like model with a long-range interaction suggested the existence of the SS in the square lattice. The above results of the SFs and the pseudo-spin correlation functions show that the state for  $c_3 > 14.3$  is a SS and it appears as a result of the interaction  $H_{NN}$ . Snapshots of the SS state in Fig.26 show that atoms are distributed rather homogeneous in the most spatial region but there also exist small domains of checkerboard symmetry. The SS state is composed of superposition of these inhomogeneous but structureless configurations.

We expect that the obtained results in this section are quite instructive for the mechanism of

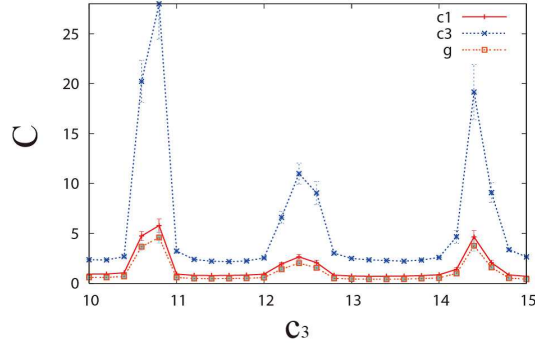


FIG. 23: Specific heat of each term as a function of  $c_3$  for  $g = 3$ ,  $c_1 = 3.0$  and  $\alpha = -0.5$ . There are three phase transitions at  $c_3 \simeq 10.8$ ,  $12.5$  and  $14.5$ .

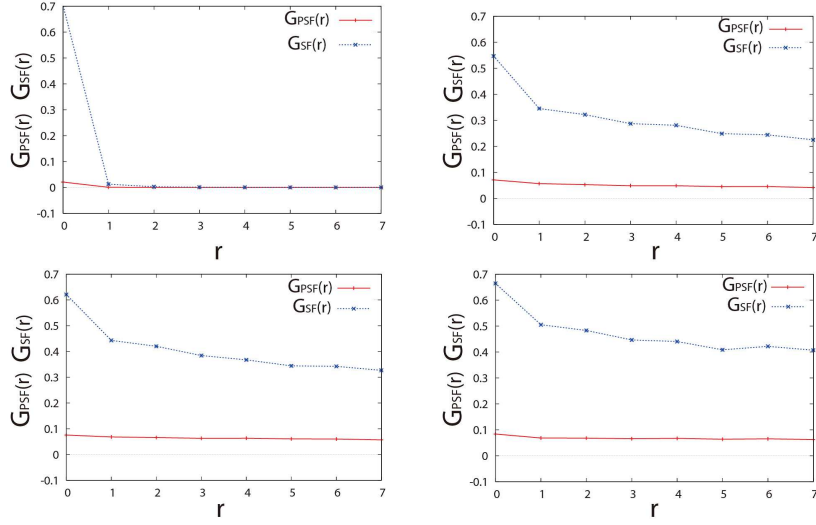


FIG. 24: Correlation functions of atoms  $G_{\text{SF}}(r)$  and  $G_{\text{PSF}}(r)$  for  $c_3 = 10$ ,  $11.5$ ,  $13.5$  and  $15$ .

the high- $T_c$  SC of the cuprates. It is expected that the single-particle SF in the bosonic t-J model corresponds to the coherent hopping of electrons in the fermionic t-J model whereas the PSF corresponds to condensation of spin-singlet electron pair at NN sites. In other words, the single-particle SF *without* the PSF corresponds to the (anomalous) metallic phase of the high- $T_c$  materials, whereas the single-particle SF *with* the PSF to the SC state. Effective attractive force appears for a pair of holes sitting on NN sites in the AF background, as the NN hole pair break eleven AF bonds, whereas two holes separating more than one lattice spacing break twelve AF bonds. It is expected that this attractive force is an origin of the high- $T_c$  SC. However the results of the present study show that the PSF does not exist in the simple bosonic t-J model, though the phase transition from the insulating AF state to the single-particle SF takes place as the hopping amplitude is increased. By adding the attractive force for particles sitting NN sites  $H_{\text{NN}}$  (5.2), the PSF is actually realized. Furthermore the resultant PSF accompanies the AF order. For the high- $T_c$  cuprates, coexistence of the AF and SC was actually observed in the recent clean materials[7]. This means that the attractive force coming from the magnetic terms in  $H_{\text{tJ}}$  is not strong enough to generate the PSF in the present bosonic t-J model. This conclusion sound rather negative for the idea of AF force for the high- $T_c$  SC. However, more precise study on difference between effect of coherent fermion hopping and BEC

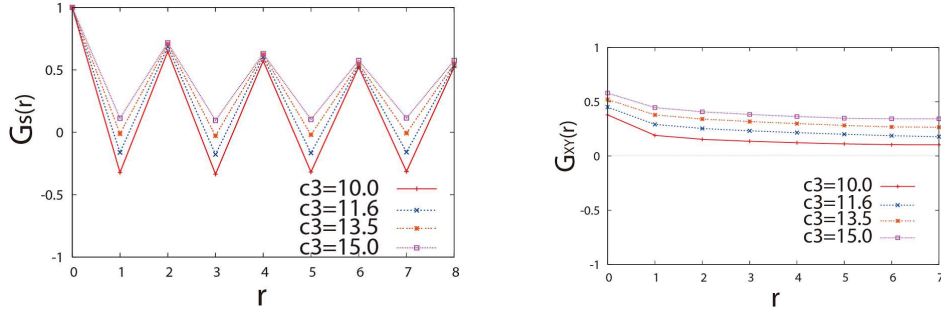


FIG. 25: Correlation functions of pseudo-spins in each phase of model  $g = 3$ . There exists AF correlation in  $z$ -component, and also FM correlation in  $xy$ -component.

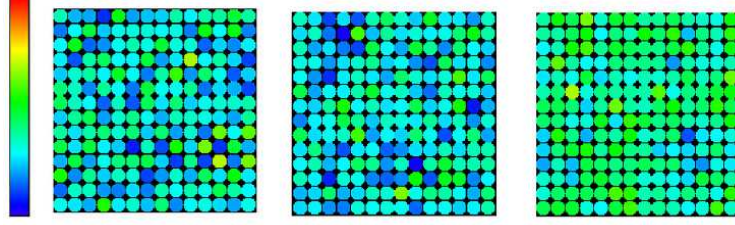


FIG. 26: Snapshots of density of  $a$ -atom (Left),  $b$ -atom (Center) and hole (Right) for  $c_3 = 15$  and  $g = 3$ .

is desired.

## VI. CONCLUSION

In this paper we have studied the three-dimensional bosonic  $t$ -J model at finite  $T$ . This model corresponds to the large on-site repulsion limit of the two-band Hubbard model. We are particularly interested in the case of the fractional filling of atoms and investigated the phase structure. We studied the model both in the GCE and CE and found that the model has a very rich phase structure. Besides the AF crystal, SF and SP state of the hetero-structure, there exist the inhomogeneous state with SF cloudlet in the AF crystal and vice versa. We found that hetero-structure of the AF crystal and SF has a sharp interface. From this observation, we give an intuitive picture of the hetero-structure that is expected to be observed by experiment in Fig.27.

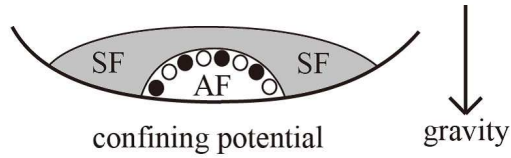


FIG. 27: Intuitive picture of hetero-structure of AF crystal and SF, which is expected to be observed by experiment.

We also studied the effect of the NN attractive force between  $a$  and  $b$  atoms. We found that in certain parameter region there appears the SS and also PSF. We think that this result gives an important insight into mechanism of high- $T_c$  SC of the cuprates.

In experiment, density and/or mass of two atoms can be varied. Then study of the cases like  $t_a \neq t_b$  and/or  $\rho_a \neq \rho_b$  is important. This problem is under study and results will be reported in a future publication.

### Acknowledgments

This work was partially supported by Grant-in-Aid for Scientific Research from Japan Society for the Promotion of Science under Grant No.20540264 and No23540301.

- 
- [1] For review, see, e.g., I. Bloch, J. Dalibard, and W. Zwerger, *Rev. Mod. Phys.* **80**, 885 (2008);  
M. Lewenstein, A. Sanpera, V. Ahufinger, B. Damski, A. S. De, and U. Sen, *Adv. Phys.* **56**, 243 (2008);  
V.I. Yukalov, *Laser Physics* **19**, 1 (2009).
  - [2] D. Jaksch, C. Bruder, J. I. Cirac, C. W. Gardiner, and P. Zoller, *Phys. Rev. Lett.* **81**, 3108 (1998).
  - [3] Y. Nakano, T. Ishima, N. Kobayashi, K. Sakakibara, I. Ichinose, and T. Matsui, *Phys. Rev. B* **83**, 235116 (2011);  
Y. Nakano, T. Ishima, N. Kobayashi, T. Yamamoto, I. Ichinose, and T. Matsui, *Phys. Rev. A* (in press), arXiv:1111.1537.
  - [4] E. Kim and M.H.W. Chan, *Science* **305**, 1941 (2004); *Nature* **427**, 6971 (2004).
  - [5] P. Sengupta, L. P. Pryadko, F. Alet, M. Troyer, and G. Schmid, *Phys. Rev. Lett.* **94**, 207202 (2005);  
B. Capogrosso, and C. Trefzger, M. Lewenstein, P. Zoller, and G. Pupillo, *Phys. Rev. Lett.* **104**, 125301 (2010).
  - [6] S. Wessel and M. Troyer, *Phys. Rev. Lett.* **95**, 127205 (2005).
  - [7] H. Mukuda, M. Abe, Y. Araki, Y. Kitaoka, K. Tokiwa, T. Watanabe, A. Iyo, H. Kito, and Y. Tanaka, *Phys. Rev. Lett.* **96**, 087001 (2006).
  - [8] A. Kuklov, N. Prokof'ev, and B. Svistunov, *Phys. Rev. Lett.* **92**, 030403 (2004).  
C. Menotti and S. Stringari, *Phys. Rev. A* **81**, 045604 (2010).
  - [9] M. Boninsegni, *Phys. Rev. Lett.* **87**, 087201 (2001); *Phys. Rev. B* **65**, 134403 (2002).
  - [10] For the bosonic t-J model on a square lattice at  $T = 0$ , see M. Boninsegni and N. V. Prokof'ev, *Phys. Rev. B* **77**, 092502 (2008). Some comments on three-dimensional system are also given there.
  - [11] S. B. Papp, J. M. Pino, and C. E. Wieman, *Phys. Rev. Lett.* **101**, 040402 (2008).
  - [12] Y. Ishibashi and M. Iwata, *Jpn. J. Appl. Phys.* **37**, L985 (1998);  
H. Fu and R. E. Cohen, *Nature* **403**, 281 (2000).
  - [13] See for example, K. Aoki, K. Sakakibara, I. Ichinose, and T. Matsui, *Phys. Rev. B* **80**, 144510 (2009).
  - [14] K. G3ral, L. Santos, and M. Lewenstein, *Phys. Rev. Lett.* **88**, 170406 (2002);  
H.P. B3cher and G. Blatter, *Phys. Rev. Lett.* **91**, 130404 (2003);  
J. M. Sage, S. Sainis, T. Bergeman, and D. DeMille, *Phys. Rev. Lett.* **94**, 203001 (2005).